Neuroscience 128 (2004) 251–262

REMODELLING OF SYNAPTIC MORPHOLOGY BUT UNCHANGED SYNAPTIC DENSITY DURING LATE PHASE LONG-TERM POTENTIATION (LTP): A SERIAL SECTION ELECTRON MICROGRAPH STUDY IN THE DENTATE GYRUS IN THE ANAESTHETISED RAT

V. I. POPOV,[a,b] H. A. DAVIES,[a] V. V. ROGACHEVSKY,[b] I. V. PATRUSHEV,[b] M. L. ERRINGTON,[c] P. L. A. GABBOTT,[a] T. V. P. BLISS[c] AND M. G. STEWART[a]*

[a]*The Open University, Department of Biological Sciences, Milton Keynes MK7 6AA, UK*

[b]*Institute of Cell Biophysics, Russian Academy of Sciences, Pushchino 142290, Russia*

[c]*Division of Neurophysiology, National Institute for Medical Research, Mill Hill, London NW7 1AA, UK*

Abstract—In anaesthetised rats, long-term potentiation (LTP) was induced unilaterally in the dentate gyrus by tetanic stimulation of the perforant path. Animals were killed 6 h after LTP induction and dendritic spines and synapses in tetanised and untetanised (contralateral) hippocampal tissue from the middle molecular layer (MML) were examined in the electron microscope using stereological analysis. Three-dimensional reconstructions were also used for the first time in LTP studies *in vivo*, with up to 130 ultrathin serial sections analysed per MML dendritic segment. A volume sampling procedure revealed no significant changes in hippocampal volume after LTP and an unbiased counting method demonstrated no significant changes in synapse density in potentiated compared with control tissue.

In the potentiated hemisphere, there were changes in the proportion of different spine types and their synaptic contacts. We found an increase in the percentage of synapses on thin dendritic spines, a decrease in synapses on both stubby spines and dendritic shafts, but no change in the proportion of synapses on mushroom spines. Analysis of three-dimensional reconstructions of thin and mushroom spines following LTP induction revealed a significant increase in their volume and area. We also found an increase in volume and area of unperforated (macular) and perforated (segmented) postsynaptic densities.

Our data demonstrate that whilst there is no change in synapse density 6 h after the induction of LTP *in vivo*, there is a considerable restructuring of pre-existing synapses, with shaft and stubby spines transforming to thin dendritic spines, and mushroom spines changing only in shape and volume.

Key words: long-term potentiation, postsynaptic densities, thin-sections, three-dimensional reconstructions.

Long-term potentiation (LTP) of the perforant path in the hippocampus has been extensively studied as an easily elicited form of synaptic plasticity (Bliss and Lømo, 1973; Bliss and Collingridge, 1993), and has become the dominant model of the synaptic basis of memory formation (Abraham et al., 2002). However, its structural basis, as with that of another form of synaptic plasticity, long-term depression, remains the subject of debate (Muller et al., 2000; Sorra and Harris, 1998; Rusakov et al., 1997; Dhanrajan et al., 2003; Mezey et al., 2004).

There is evidence for LTP remodelling both at pre- and post-synaptic levels. Malenka and Nicoll (1999) have summarised the importance of the role played by changes in the number and/or properties of postsynaptic receptors. Changes in presynaptic function during long term synaptic plasticity were visualised by Zakharenko et al. (2001) using 2-photon microscopy and Emptage et al. (2003) applied optical quantal analysis to reveal a presynaptic component of LTP at hippocampal Schaffer-associational synapses. Postsynaptic mechanisms of LTP are reflected morphologically in dendritic spine remodelling (Kirov and Harris, 1999; Toni et al., 1999, 2001; Yuste and Bonhoeffer, 2001). Alterations in synapse number or in structure of dendritic spines occur as early as 30 min post LTP induction (Desmond and Levy, 1986a,b, 1988, 1990) and last for hours to days (Geinisman et al., 1991, 1994; Stewart et al., 2000).

Confocal microscopy has provided three-dimensional (3D) representations of dendritic spines and presynaptic boutons (Engert and Bonhoeffer, 1999; Segal, 2001) but there are limitations in using confocal microscopy alone, especially in the study of presynaptic elements (Harris, 1994; Moser et al., 1997). Single-section analysis of electron microscope sections can also be problematical because variability in synapse density and morphology substantially influences the probability of viewing structures on random single sections (Coggeshall and Lekan, 1996; Fiala and Harris, 2001a).

Sorra and Harris (1998) used 3D synaptic reconstructions to show that LTP induced *in vitro* did not result in formation overall of new synapses at 2 h post-tetanus in hippocampal area CA1. Their study supported the hypothesis that early phase LTP involved a redistribution of synaptic weights amongst pre-existing synapses,

*Corresponding author. Tel: +44-1908-653448; fax: +44-1908-654167.
E-mail address: m.g.stewart@open.ac.uk (M. G. Stewart).

Abbreviations: DG, dentate gyrus; EM, electron micrograph; fEPSP, field excitatory postsynaptic potential; LTP, long-term potentiation; MML, middle molecular layer; mPSD, macular post-synaptic density; Msp, mushroom spine; pPSD, perforated post-synaptic density; PSD, post-synaptic density; SA, spine apparatus; sPSD, segmented post-synaptic density; Tsp, thin dendritic spine; 3D, three-dimensional.

0306-4522/04$30.00+0.00
doi:10.1016/j.neuroscience.2004.06.029

in contrast to electron microscopic observations which suggested the splitting of existing spines contacting the same pre-synaptic bouton (Toni et al., 2001), and confocal studies which point to the formation of new spines after tetanic hippocampal stimulation (Engert and Bonhoeffer, 1999; Korkotian and Segal, 2001).

Here, following LTP induction *in vivo* we have examined morphological changes in spines and synapses in another hippocampal pathway, the perforant path projection to granule cells of the dentate gyrus. A detailed quantitative examination has been undertaken using stereological analysis and, for the first time in an *in vivo* LTP study, 3D reconstructions of serial ultrathin sections have been made (Harris, 1994; Fiala and Harris, 2001a; Harris et al., 2003). The perforant path in the left hemisphere was subjected to tetanic electrical stimulation whilst the right hemisphere served as an unstimulated control. In an additional control, unilateral electrical stimulation of the perforant path was employed in a pattern that did not induce LTP. Animals were killed 6 h after the induction of LTP, an interval long enough to ensure that any changes reflected the late, protein-dependent phase of LTP. Our results reveal no change in synaptic density, but a considerable remodelling of existing synapses, with thin dendritic spines (Tsp) replacing shaft and stubby spines, and mushroom spines (Msp) increasing in volume.

EXPERIMENTAL METHODS

Induction of LTP *in vivo*

Male Sprague–Dawley rats weighing 300–400 g were anaesthetised with urethane (1.8 g/kg i.p.), and held in a semi-stereotaxic apparatus. A glass recording pipette, filled with artificial cerebrospinal fluid containing Pontamine Sky Blue was placed 4.1 mm posterior and 2.5 mm lateral to bregma and advanced into the dentate gyrus (DG). A bipolar stimulating electrode (Rhodes SNE 100) was inserted on the same side 4.4 mm lateral to lambda and lowered into the angular bundle to activate fibres of the perforant path. The depths of the two electrodes were adjusted to produce maximal responses in the cell body layer. Constant current stimuli (60 μs duration, intensity in the range 70–120 μA) were delivered at intervals of 30 s, and intensity adjusted to produce a population spike with an amplitude of 1–2 mV. Test stimuli were delivered at 30-s intervals for 30 min prior to induction of LTP and for 6 h afterward. LTP was produced by three trains of 50 pulses at 250 Hz, with an inter train period of 30 s. A control animal received no tetanic stimulation but was given the same extra 150 stimuli, corresponding to the number of stimuli in the tetanus protocol, spread at equal intervals over the final 6 h of the experiment; the stimulus strength in this animal was also raised for the final 6 h to mirror the increased evoked responses produced during LTP in the potentiated animals. The collection of evoked potentials and the timing and intensity of stimulation, were under computer control (software written by Dr R. M. Douglas, University of British Columbia). All animal experimentation was carried out under UK Home Office licence, and care was taken to minimise the number of animals used and their suffering throughout all stages of the procedures.

Fixation by perfusion

Following physiological stimulation, male rats (three animals for LTP and one for electrical stimulation without LTP) were perfused intracardially. Primary fixation occurred via a two-stage process. Firstly, the thorax was opened and the left cardiac ventricle cannulated. The right cardiac auricle was then opened, and 100 ml of phosphate-buffered physiological saline was perfused through the animal. Subsequently, 100 ml of 3% paraformaldehyde and 0.5% glutaraldehyde in 0.1 M Na-cacodylate buffer (pH 7.2–7.4) was perfused transcardially at room temperature. In the second stage the hippocampus was removed, and cut into 300 μm slices and fixed in a higher concentration of glutaraldehyde, as described below.

Hippocampal volume

The volume of the left and right hippocampi were estimated by using the Cavaleri method (Pakkenberg and Gundersen, 1997; Stuart and Oorschot, 1995). Three rats were tetanized exactly as above with a recording electrode in the left, tetanised hemisphere, and another recording electrode in the DG of the right unstimulated hemisphere. After 6 h, the animals were transcardially perfused with aldehyde fixative (as described above) and the brains carefully removed and stored in 0.1 M PB (pH 7.4). The fixed brains were then serially sectioned in the coronal plane at 100 μm (section thickness, t) on a vibrating microtome (Leica). Tissue sections were mounted in order on glass slides, air dried and subsequently stained with a solution of 0.1% Toluidine Blue in 0.1 M PB buffer (pH 7.4) for 2 min. Sections were then washed, dehydrated in an ascending series of alcohols, passed through xylene and finally embedded in DPX. From the complete rostrocaudal set of sections in each animal a 1:3 series was selected for analysis. Sections were viewed and analysed at low magnification in a Nikon E600 digital photomicroscope. Using previously published cytoarchitectonic criteria (Swanson, 1998), the boundaries of the DG (cell body layer and molecular layer) and of the total hippocampus (including CA1, CA2, CA3, DG, polymorph cell and hilar regions, but excluding the subiculum) were defined bilaterally in each rostrocaudal section (Fig. 1A). Bilateral digital images including the hippocampus and surrounding structures were captured electronically and displayed on a computer screen (Fig. 1A). No gross cytoarchitectural differences were detected between control (right) and tetanised (left) hemispheres. The surface areas of the dentate gyri and of the whole hippocampi occurring in each section of the 1:3 series were then calculated using a calibrated measuring programme (Lucia Version 4.8; Laboratory Imaging Ltd., Prague, Czechoslovakia; Fig. 1B). Total hippocampal and total dentate gyral volumes for each hemisphere were subsequently derived by multiplying the total surface areas of each structure in each analysed section by the number of sections in the series ($n=3$) and by the section thickness (t). Data are presented as mean±S.D. Statistical comparisons in volume data between regions, hemispheres and animals were performed using multiple *t*-tests.

Electron microscopy

After perfusion with fixatives as described above hippocampi were dissected out and slices approximately 300 μm thick were cut transverse to the long axis of the dorsal hippocampus. Four slices were taken from each animal 1–2 mm on either side of the electrode tract in the tetanized hemisphere and four slices from a similar location in the contralateral hemisphere. The slices were fixed further by immersion in 0.1 M Na-cacodylate buffer (pH 7.2–7.3) containing 2.5% glutaraldehyde for 1–2 h at room temperature, followed by three washes in cacodylate buffer. The tissue was post-fixed with 1% osmium tetroxide and 0.01% potassium dichromate in cacodylate buffer for 1–1.5 h at room temperature.

Processing for microscopy

Tissue was dehydrated in aqueous solutions of ethanol at 40, 50, 60, 70, 80 and 96% (each for 10 min) and 100% acetone (three changes,

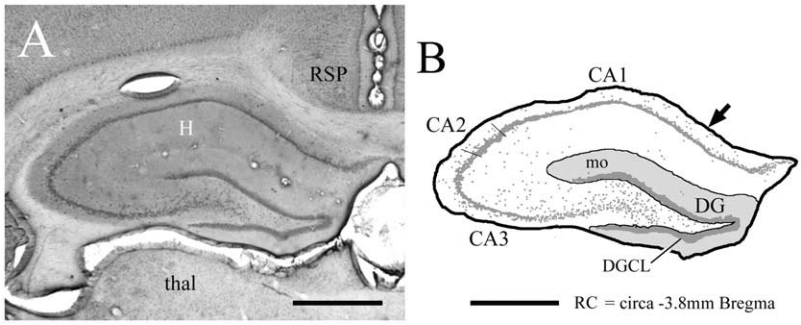

Fig. 1. Definition of hippocampal regions. (A) Toluidine Blue-stained section (100 μm thick) showing the dorsal hippocampus (H) on the 'tetanised' left side. Neighbouring regions are indicated (RSP, posterior retrosplenial cortex; thal, thalamus). Section viewed from anterior pole and taken along rostrocaudal (RC) axis at approximately −3.8 mm from Bregma. (B) Line drawing of section shown in A indicating the perimeter boundary (black arrow-thick black outline) defining the whole hippocampus at this RC level. Also shown is the region designated as the DG. DGCL is defined as the combined dentate granule cell layer (gcl, dark grey) and the molecular layer (mol, light grey). Scale bar=1 mm (A and B).

each for 10 min). Specimens were infiltrated with a mixture of 50% epoxy resin, 50% pure acetone for 30 min at room temperature. Each slice was placed on a Teflon support and covered with a capsule containing pure epoxy resin (Epon 812/AralditeM epoxy resin) for 1 h at 60 °C and polymerised overnight at 80 °C. Slices in blocks were coded and all further analyses were carried out with the investigator blind to the experimental status of the tissue. The embedded slices on the block surface were trimmed with a glass knife along the entire surface of the hippocampal slice and 1–2 μm-thick sections cut. The sections were stained with Toluidine Blue and examined in a light microscope. Using a glass knife a trapezoid area was prepared, with one side of 20–25 μm in length, and including area CA1, fimbria, DG and area CA3/CA4. Serial sections were cut with a Diatome diamond knife and allowed to form a ribbon collected on the surface of a water/ethanol solution (2–5% ethanol in water) in the knife bath. A ribbon of serial sections was collected on pioloform-coated slot grids and counterstained with saturated ethanolic uranyl acetate, followed by Reynolds lead citrate (15–20 min each). Fig. 2 illustrates the trapezoid area as cut from the block. Grids were placed in a rotating grid holder to obtain uniform orientation of sections on adjacent grids. Sections were examined with a JEOL 1010 electron microscope and photographed at 6000× magnification. A grating replica (d=0.463 μm; Electron Microscopy Sciences Inc., Fort Washington, PA, USA) was used for calibration of electron microscope magnifications. A cross-sectioned myelinated axon or dendrite spanning all sections provided a fiduciary reference for initial alignment of serial sections. Section thickness was determined using the approach of Fiala and Harris (2001b) and was normally of 60–70 nm-thickness (grey-white colour); approximately 90–130 serial sections were collected per series from each block.

Stereology of synapses

Stereological estimates were made of synapse density. We selected for analyses the middle molecular layer (MML) which is the main target area of perforant path fibres; the regions analysed were 60–100 μm (MML), from the proximal edge of the granule cell layer. Stereological analysis was performed according to Harris (1994; Fiala et al., 1998; Sorra et al., 1998), with tissue volumes of approximately 500–800 cubic micrometers. Synaptic number was counted within these areas irrespective of the presence of components such as large dendrites on the grounds that to do so would have potentially biased data obtained. Synaptic densities were expressed as number of synapses (identified via PSDs), per 100 μm^3 of tissue.

Digital reconstructive analysis

Digitally scanned electron micrograph (EM) negatives with a resolution of 900 dpi were aligned as JPEG images (software available from Drs. Fiala and Harris: http://synapses.bu.edu). Alignments were made with full-field images. Contours of individual dendrites, axons, dendritic spines, PSDs, and mitochondria were traced digitally and volumes, areas, and total numbers of structures, were computed.

Statistical analysis

Microcal Origin software was used to plot graphs, to obtain means and S.D.s, and to perform tests of significance, as described in the results. ANOVAs followed by Tukey's unequal N honest significant differences tests. Data are presented as a mean±S.D.). Significance levels were set at $P<0.05$.

RESULTS

Volume measurements

In order to interpret changes in synaptic density, derived from stereological analysis of EM sections, in terms of changes in synaptic number, we first determined whether the induction of LTP causes any change in volume of the DG.

All rats stimulated exhibited potentiation of the synaptic response that was more than 20% above the pre-tetanus level. The slope of the field excitatory postsynaptic potential (fEPSP) was normalised to the mean value before the tetanus for each animal, and group means are shown for the two groups of animals (three used for EM, and three for estimates of volume changes associated with LTP; Fig. 3).

The volumes of the DG and the combined hippocampal subfields are given in Table 1 for the tetanised and unstimulated hemispheres of each of the three rats. As can be seen by comparing the tetanised and untetanised hemispheres, the induction of LTP in perforant path–granule cell synapses had no statistically significant effect on the volume of the hippocampus or DG.

Ultrastructural analysis

Each synapse was identified primarily on the basis of the presence of a post-synaptic density (PSD) with vesicles in close proximity to the pre-synaptic zone. There are two main categories of PSDs: macular (with a continuous PSD) and those with a perforation in the PSD (perforated). Segmented PSDs are a subset of perforated PSDs (Sorra and Harris,

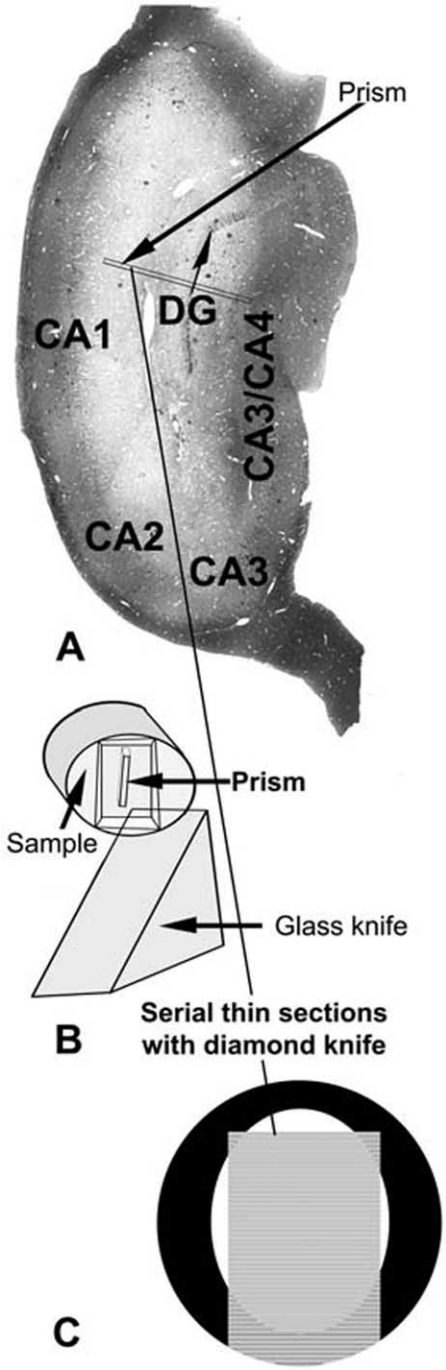

Fig. 2. Section cutting: (A) Sections were cut from the hippocampal blocks using a trapezoid to include CA1, dentate and CA3/4 (A). (B) The trapezoid is 25 μm in length but is very narrow in breadth. (C) Trimming was carried out with a glass knife but ultrathin serial sectioning was carried out by a diamond knife and section ribbons are collected on slot grids.

1998). In the present investigation PSDs located on dendrites originating from non-spiny interneurons (Harris, 1994) were ignored. Fig. 4A–D shows four non-consecutive serial EMs from a series of 130 sections. Fig. 4E–G are 3D-reconstructions from this series, taken from the MML of the potentiated DG (approximately 80–100 μm from the border of granule cell bodies) aligned as described above using IGL Trace software; macular and segmented PSDs are present. Fig. 4A, B (EM numbers 21 and 23) shows a dendrite (D) and four thin spines (sp 1, 2, 3 and 4) and their associated macular synaptic zones which consist of both the pre-synaptic and post-synaptic electron densities. These sections together with others from the series (not shown) produced the dendritic reconstruction shown in Fig. 4E (in two rotational positions), with the PSDs indicated in red. Fig. 4C, D shows EM numbers 28 and 31 of the series from the same dendritic segment. These contain a perforated/segmented PSD (pPSD) on a Msp, indicated by the asterisk in both EM numbers 28 and 31. The stalk of the spine is also shown. Note that in EM number 31 there is a spinule protruding from the PSD into the pre-synaptic bouton and a spine apparatus (SA) can be seen in the spine head. The spine and PSD together with the pre-synaptic density seen in EMs 28 and 31 are shown reconstructed in three dimensions in Fig. 4F, which is composed of other sections (not shown) from the same series. The segmented form of the PSD (red) together with the spinule is clearly seen in this reconstruction, as is the concave form of the spine head.

Only axo-spinous and shaft synapses were analysed in this study. Four categories of synapses were subjectively classified according to their post-synaptic contact, three according to whether the dendritic spine was 'mushroom,' 'thin,' or 'stubby.' The fourth category comprised synapses in which the presynaptic bouton contacted the dendrite directly and was termed a 'shaft' synapse. Although there is no absolute classification of thin and mushroom (M)sps, a spine was classified as *mushroom* if its head was appreciably wider than the width of the neck (as in Fig. 4F); *thin*, if its length was greater than the width of its neck and head, and *stubby*, if the width of the neck was similar to its length (Peters and Kaiserman-Abramof, 1970). Generally here, the volume of a thin spine was approximately 10 times less than the volume of a Msp. Examples of the four categories are shown in Fig. 4G, which is a complete reconstruction of over 130 serial ultrathin sections of a dendritic segment from the MML (a different series from that shown in Fig. 4E, F); PSDs, both macular (mPSD) and segmented (sPSD) are shown in red. A diagrammatic representation of the four categories of synapse is shown in Fig. 4H.

Synapse density: Stereological analysis

Stereological measurements of synapse density in the MML were made from: (i) potentiated (left) and (ii) unstimulated (right) hemispheres of the tetanised rats, and (iii) from the stimulated but unpotentiated (left) and unstimulated (right) hemispheres of the control rat. No distinction was made between synapse type (macular or perforated/segmented), or the nature of the spine contact when calculating overall synaptic density. Individual synaptic density values for each of the three tetanized hemispheres, and the three contralateral hemispheres showed little variation, and when the mean synaptic densities (Fig. 5A) were estimated, these showed no differences between the three groups (one-way ANOVA, $P>0.05$):

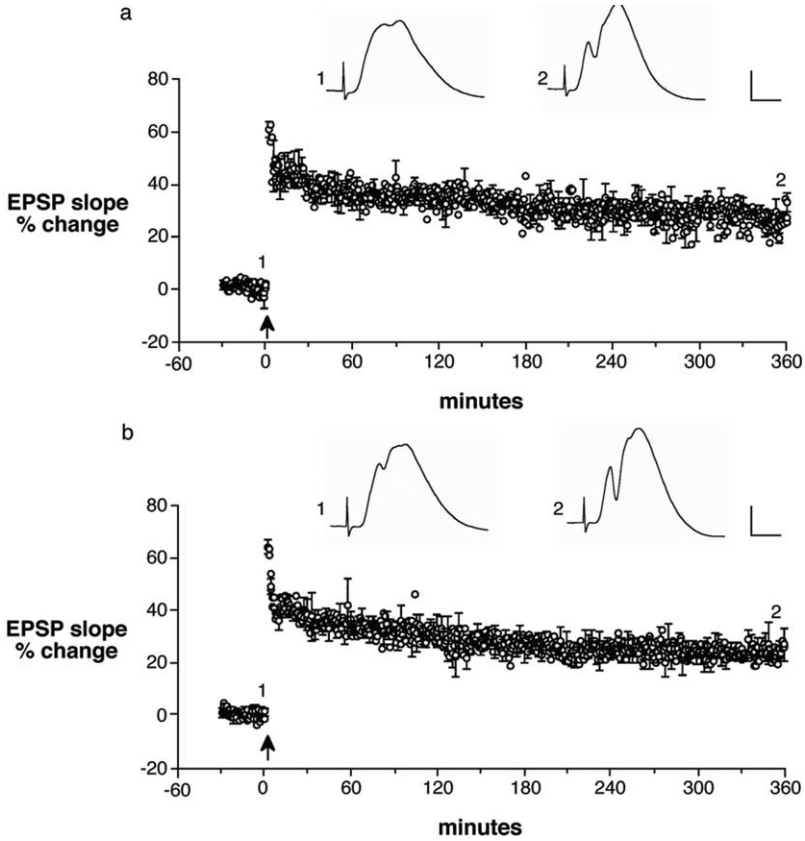

Fig. 3. Time course of LTP. (a) Mean slope of the fEPSP measured in the hilus of the DG on stimulated side, normalised with respect to the mean slope before high-frequency stimulation (arrow), for the three animals used to examine possible volume changes in the DG following the induction of LTP. Sample field potentials recorded immediately before and up to 6 h after the induction of LTP are displayed above the graph. (b) Similar graph and sample potentials plotting the mean fEPSP in three different animals whose brains were used for electron microscopy. Calibrations: 4 msec, 4 mV.

(i) 303±20 per 100 μm^3 in the right (unstimulated) hemisphere (hippocampi from three animals, with three serial section series consisting of 75–95 serial thin sections; 500 synapses were counted);
(ii) 315±26 per 100 μm^3 in the potentiated hemispheres (hippocampi from three animals; five serial section series consisting of 82–130 serial sections; 750 synapses counted);
(iii) 303±28 per 100 μm^3 in the stimulated but not potentiated hemisphere of the control rat (one animal; three serial section series consisting of 73–94 serial sections; 450 synapses were counted).

Percentages of the four categories of synapses (contacting spines or shafts) in the MML of potentiated and control tissue: Serial section analysis and 3D reconstructions

The possibility of synaptic or dendritic spine remodelling cannot easily be ascertained from the stereological

Table 1. LTP is not associated with a change in the volume of dentate gyrus in the tetanized hemisphere[a]

	Untetanised		Tetanised	
	R-DG	R-total Hippocampus	L-DG	L-total Hippocampus
Mean volume	8.63±0.50	30.53±3.88	8.53±0.93	31.70±3.50
Volume ratio (DG/sum hippo %)	28.5±3.82		26.9±1.91	

[a] Mean volumes (±S.D.) in mm^3 of the left (L) and right (R) hippocampi and left (tetanised) and right (untetanised) DG estimated by use of the Cavaleri method. The boundaries of the DG (cell body layer and molecular layer) and of the total hippocampus (including CA1, CA2, CA3, DG, polymorph cell and hilar regions, but excluding the subiculum) were defined bilaterally in each rostrocaudal section (see Fig. 1A). Total hippocampal and total DG volumes for each hemisphere were derived by multiplying the total surface areas of each structure in each section by the section thickness (t). Statistical comparisons in volume data between regions, hemispheres and animals were performed using multiple *t*-tests. There are no significant differences between hemispheres, nor between whole hippocampus and dentate gyrus, or for the volume ratios of DG:hippocampus. Hippo, hippocampus.

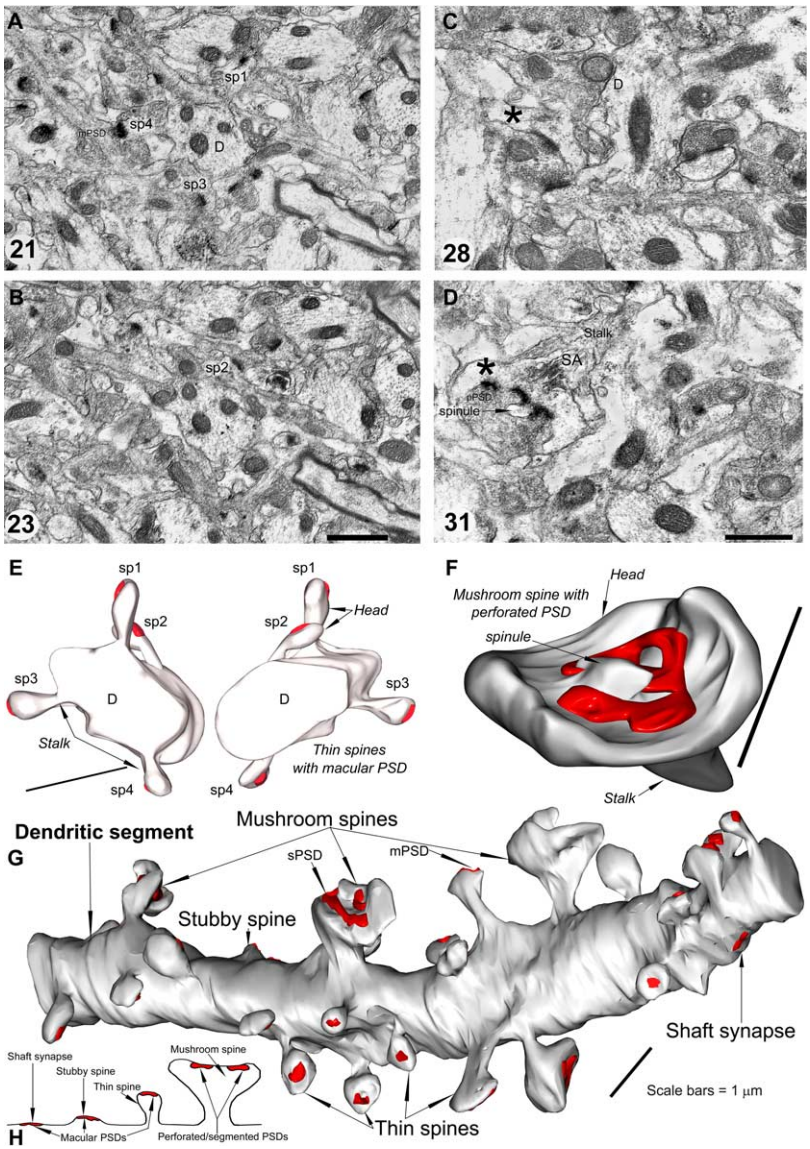

Fig. 4. Classification of spines and synapses in the medial perforant path terminal zone. Four EMs and 3D reconstructions from a series consisting of up to 130 sections from the MML of the hippocampus (approximately 80–100 μm from the border of the granule cell layer) 6 h after the induction of LTP, aligned using IGL Trace software. All images were scanned at 900 dpi resolution and saved in JPG format (approximately 9 Mb file size): initial EM magnification was 6000×. PSDs in the reconstructions are shown in red. (A, B) EM sections 21 and 23 of a series consisting of 130 serial sections, showing a dendrite (D) and four thin spines (sp 1, 2, 3 and 4) with mPSDs. (C, D) EMs 28 and 31 of the same series. These show a pPSD on a Msp, indicated by the asterisk in EMs 28 and 31. The stalk of the spine is also indicated. Note that in EM 31 there is a spinule protruding from the PSD into the pre-synaptic bouton and a SA in the spine head. Scale bar=1.0 μm. (E) 3D reconstructions (in two rotational positions) from the series illustrated in A–D, with thin spines and the PSDs indicated in red. Scale bars=1.0 μm. (F) The spine and PSD seen in EMs 28 and 31, reconstructed in 3D, showing it as a Msp. The sPSD (red) is clearly seen in this reconstruction, as is the concave form of the spine head. Scale bar=1.0 μm. (G) Example of a complete reconstruction of 130 serial sections of a different dendritic segment from the MML showing examples of the four synapse/spine categories used in this study mushroom (Msp) thin (Tsp), Tsp or stubby spines, or as synapses directly on the dendritic shaft (spines classes as defined by Peters and Kaiserman-Abramof, 1970). PSDs are red (sPSD and mPSD). Scale bar=1.0 μm. (H) A diagrammatic representation of the four spine categories, as indicated in G with PSD (red).

measurements presented in Fig. 5A. Accordingly, 3D reconstructions were performed on serial sections (up to 130 per reconstruction) taken at random from the MML. Sufficient reconstructions were made to obtain a minimum of 100 of each the four categories of synapse in each of the potentiated, unstimulated, and stimulated but not potentiated states. The number of synapses per unit area is presented in Fig. 5B as percentages of the total number of synapses. The percentage of thin spines is significantly increased ($P<0.01$) in the MML of the DG of the potentiated hemisphere compared with either the equivalent region in the unstimulated contralateral hemispheres or in the stimulated but not potentiated hemisphere of the control rat. Conversely, the percentage of both stubby and shaft synapses decreased significantly ($P<0.01$) in the potentiated hemisphere compared with

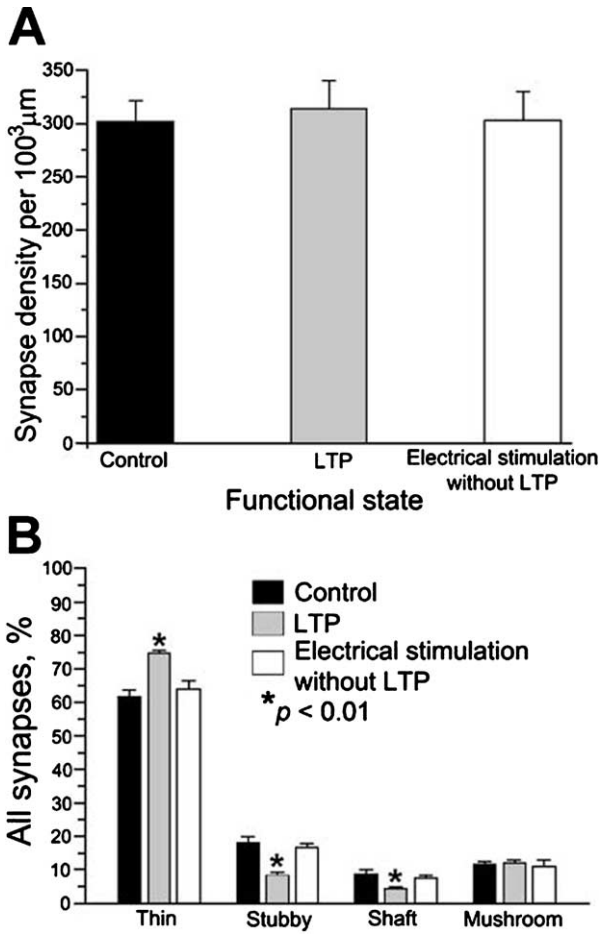

Fig. 5. LTP is not accompanied by a change in overall synapse density. Morphometric parameters from stereological analyses of synapses and dendritic spines in the MML of the dentate 6 h after induction of LTP *in vivo*. The analyses include examination of sample fields from the MML of the DG for three functional states: control (tissue from unstimulated hippocampi from the right hemisphere of three animals, 12 samples); LTP (tetanised hippocampi from the left hemisphere of the same three animals, 6 h post-induction; 12 samples); and electrical stimulation without LTP (six samples from left stimulated hippocampus. Data are expressed as mean±S.D.). (A) The number of synapses (PSDs) per 100 μm^3 of DG. There are no significant differences between the three functional states. (B) Distribution of the four categories of synapses (those on Tsp, stubby and Msps, and those on dendritic shafts), expressed as percentages of the total number. Following LTP there is a significant increase in the proportion of synapses on Tsps and a concomitant decrease of stubby and shaft synapses ($P<0.01$). The proportion of Msp synapses is unchanged between the three control and LTP hemispheres.

the unpotentiated hemispheres, whilst the percentage of Msps remained unchanged.

Thin spines (Tsps)

Two Tsp are shown in an EM Fig. 6 (left), and representative examples from reconstruction of serial sections in Fig. 6A, B. Comparative qualitative analysis of 3D images suggests that the shape of the spine heads is more concave in potentiated than unpotentiated tissue (compare Fig. 6A and B). A plot of the distribution of volume of thin spines in the middle third of the molecular layer of potentiated and unpotentiated tissue (Fig. 7A) shows a pronounced shift toward spines with a larger volume following the induction of LTP (increase in mean volume 92%, $P<0.001$, and in mean area 53%, $P<0.001$). The pre- and post-synaptic densities were neither perforated nor segmented in thin spines, all being macular in appearance. Quantitative measurements of volume and area of mPSDs of thin spines (Fig. 7B) showed a two-fold increase in these parameters following the induction of LTP (for both $P<0.001$).

Mushroom spines (Msp)

Two Msp are shown in an EM in Fig. 6 (left). Examples of randomly selected Msps from control and potentiated tissue are displayed in Fig. 6C and B, respectively. As with thin spines, tetanic stimulation appears to induce a shape change in the spine head. Six hours after the induction of LTP (Fig. 6D) the spine heads have a notably more concave shape in contrast to the flatter or even convex shape of the spine head in unstimulated tissue (Fig. 6C).

Fig. 7C (and inset values) shows that induction of the LTP results in significant increases in both volume (42%, $P<0.01$), and area (30.5%, $P<0.01$) of Msps, whilst there are also significant increases in the volume (38%, $P<0.01$) and area (21%, $P<0.01$) of the PSDs on these spines (Fig. 7D).

The overall impact of LTP induction on all classes of dendritic spines is shown in Fig. 7E; there are significant increases in volume (185%, $P<0.01$) and area (44%, $P<0.01$). The volume and area of PSDs of all synapse types, irrespective of the nature of their spine contact, is shown in Fig. 7F, with volume increasing after LTP by 47% ($P<0.01$) and area by 32% ($P<0.01$).

DISCUSSION

This is the first detailed 3D reconstruction study of changes in synaptic and dendritic spine morphology associated with late LTP *in vivo*. In order to ensure that our morphometric estimations were not influenced by volume changes of hippocampal tissue we have compared the volumes of both hippocampus and DG in each hemisphere and have confirmed that there are no significant differences in tissue volume following the unilateral induction of LTP. This lends strong support to the conclusion that our stereological measurements, showing no change in synapse density per unit volume of tissue the DG 6 h after the induction of LTP, can be interpreted as indicating no change in the number of synapses in the regions measured. However, 3D reconstructions of serial sections demonstrate that LTP is associated with significant changes in the size and shape of the synaptic density specialisations, in particular the PSD volume of which we have measured, and in the proportion of the different types of spines.

The finding that induction of LTP in the DG *in vivo* does not lead to a change in synapse number 6 h after the tetanus is consistent with the conclusion reached by Sorra and Harris (1998) in their analysis of synapse number in area CA1 2 h after the induction of LTP *in vitro*. Changes

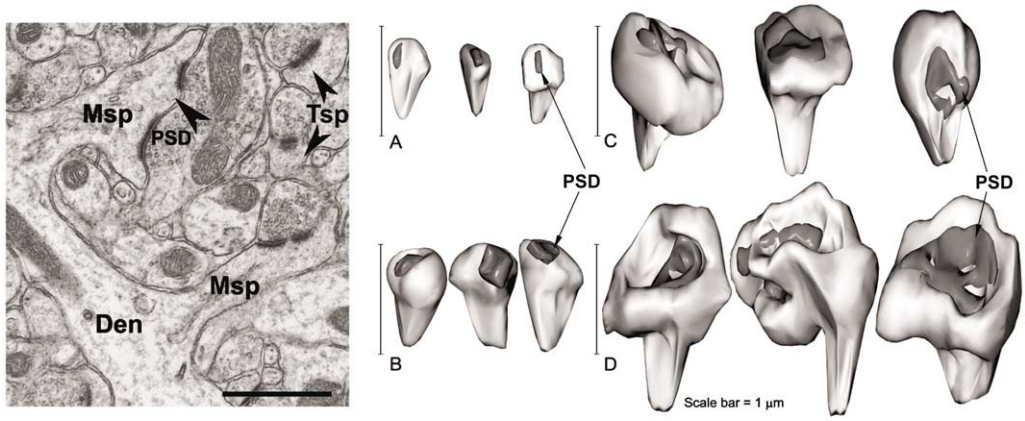

Fig. 6. LTP is associated with an increase in the spine volume and in the concavity of PSDs. (Left) EM showing an example of thin (Tsp) and mushroom (Msp) dendritic spines: both spine types are contacted by synapses with asymmetric synaptic apposition zones and prominent PSDs which are thicker than the presynaptic area, hence they are termed asymmetric synapses. Both PSDs on the Msps are perforated, indicated by the arrow head in the PSD of the synapse on one of the Msps. The Msps can be seen clearly to originate from a dendrite (Den). Scale bar=1.0 μm. (A) 3D reconstructions of three Tsps and PSDs (grey, indicated by arrows), from control tissue. The spines were selected as representative of those from this category in the MML. PSDs are all macular, which is typical of Tsps. (B) Examples of 3D reconstructions of three Tsps and PSDs 6 h after induction of LTP. Induction of LTP leads to an increase in both volume and area of Tsps. (C) 3D reconstructions from the control hemisphere (MML) showing three examples of Msps. Both perforated and sPSDs (grey, arrows) are illustrated. Spine heads are relatively flat in shape. (D) After induction of LTP, the Msp heads have a relatively concave shape and the PSDs (grey) are considerably enlarged. Scale bars=1 μm (A–D).

in synaptic structure and number are likely to depend critically on the post-induction interval since the phase of LTP which requires enhanced protein synthesis (both *in vivo* and *in vitro*) begins 2–5 h after induction of potentiation (Frey et al., 1988; Frey and Morris, 1997), arguing that more prominent structural changes, if any, are likely to occur after this period. Hence comparisons of morphometric parameters from different laboratories need to consider the time after tetanisation at which the analyses were performed. Previous data from one of our laboratories (Stewart et al., 2000) indicated an increase in synapse density after induction of hippocampal LTP *in vivo*. However those data were obtained 24 h after stimulation, and used analyses based upon a two-section disector, rather than 3D reconstructions. We cannot conclude that the restructuring observed here 6 h after induction precludes changes in synapse density in the MML at other times. Nor can we rule out the possibility suggested by Sorra and Harris (1998) that both synaptogenesis and synapse elimination occur, resulting in no net change in synapse number or size.

Significant increases also occur in total volume and area of the 3D reconstructed spines following LTP induction, and in the volume and surface area of the postsynaptic density. Unperforated (macular) synapses were almost all located on thin spines whereas synapses with perforated/segmented junctions occurred on Msps; the volume and area changes occurred in both types of synapse. An increase in the area of the PSD may reflect a role in enhanced synaptic efficacy, perhaps through the accommodation of additional receptors (Malenka and Nicoll, 1999), and/or an increase in the population of recycling vesicles as discussed by Marrone and Petit (2002). Although we have not made quantitative measurements our data appear to show qualitatively that LTP is associated with an alteration in size and shape of the PSD, together with a transformation in the shape of the spine head from relatively flat or convex to a more concave form in potentiated tissue, as also observed by Weeks et al. (1999, 2000, 2001, 2003) in the DG of the freely moving rat. If our qualitative observations are correct they would support earlier findings by Desmond and Levy (1983), determined by single section analysis for DG *in vivo*, and in hippocampal slices for area CA1 (Chang and Greenough, 1984) and CA3 (Petukhov and Popov, 1986). As controls we have used: (i) the unstimulated hemispheres and (ii) a stimulated but untetanised hemisphere. The changes we observed in the anaesthetized animal are therefore attributable to tetanic stimulation. The LTP-associated changes in the incidence of concave synapses reported by Weeks et al. (2003) in the DG of the unanaesthetised rat were not seen when the induction of LTP was blocked with ketamine, a competitive NMDA antagonist. We conclude that our results reflect the induction of LTP, rather than nonspecific changes related to tetanic stimulation, or to an interaction between anesthesia and tetanic stimulation.

The alterations in the proportions of the four categories of synapse (on thin, stubby and mushroom spines, and on dendritic shafts) 6 h after the induction of LTP result from a significant increase in the proportion of synapses on thin spines and a concomitant decrease in synapses on shaft and stubby spines. In contrast, the proportion of Msp synapses is unchanged after LTP though the area of perforated synaptic densities on Msps increases significantly, as does their volume.

Our interpretation of the changes in synapse and spine structure 6 h after the induction of LTP *in vivo* is illustrated diagrammatically in Fig. 8. LTP is accompanied by a transition from stubby spines and shaft synapses to thin spines (Fig. 8(1)), with an overall increase in the length of thin spines (Fig. 8(2)). In thin spines the mPSD becomes larger and appears more concave as

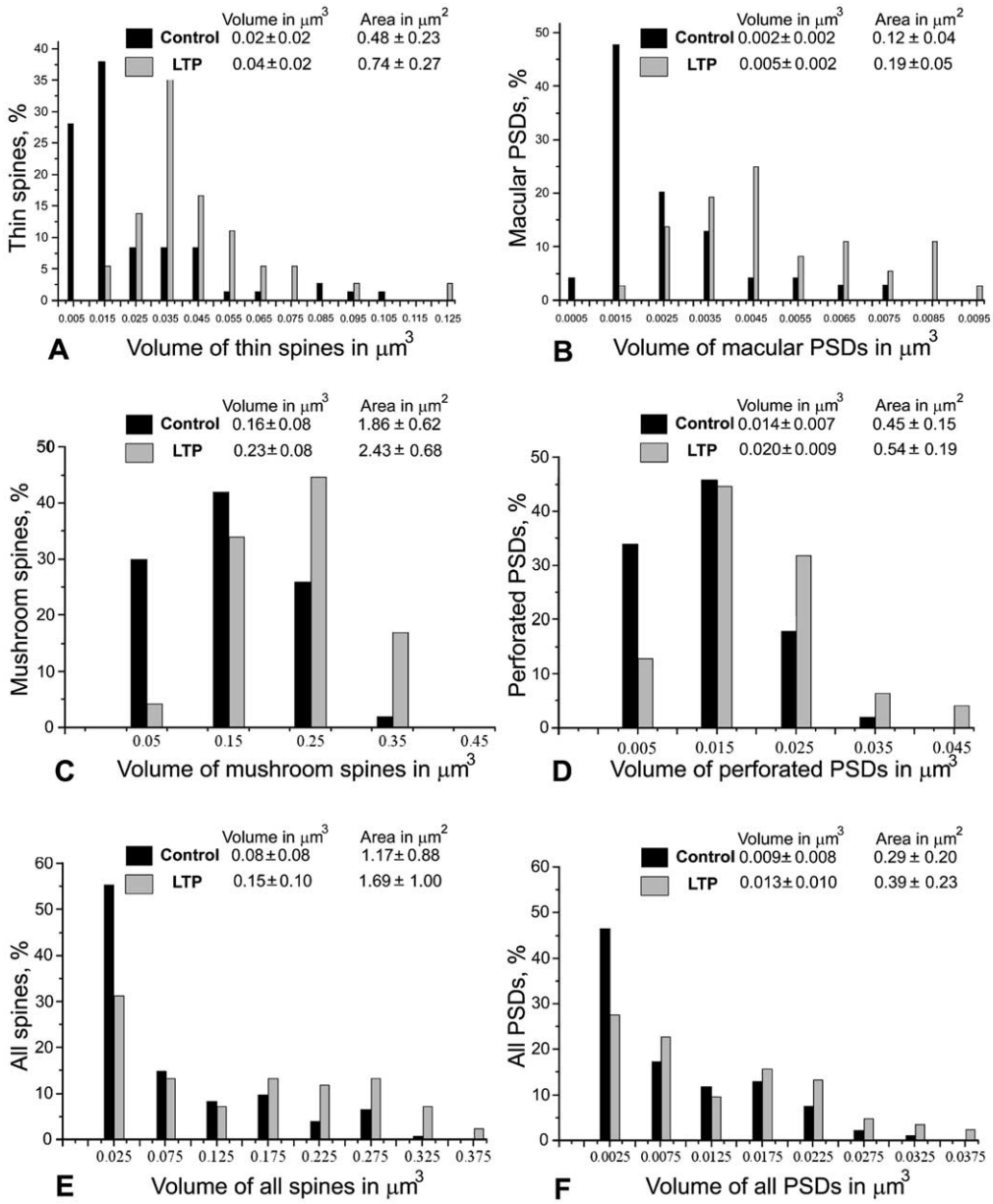

Fig. 7. LTP is associated with an increase in spine volumes. Morphometric parameters derived from 3D reconstructions of synapses and dendritic spines in the MML of the DG 6 h after induction of LTP *in vivo*. The analyses include 12 sample fields for each of two states, control (tissue from unstimulated hippocampi from the right hemisphere of three animals), and LTP (tissue from tetanised hippocampi from the left hemisphere of the same three animals, 6 h post-induction). The distributions are presented as percentages of the total number of spines or PSDs that fell in each size interval. Mean data (volume and area for each measure±S.D.) are also tabulated in the insets to each panel. (A) Distribution of volume of Tsp, in control tissue (black column) and potentiated tissue (grey column). The volume of 3D reconstructed Tsps is grouped in steps of 0.01 μm^3. LTP is accompanied by a significant increase in volume and area of Tsps ($P<0.001$). (B) Distribution of volume of mPSDs in control and potentiated tissue. The volumes of mPSDs, computed from 3D reconstructions, are grouped in steps of 0.001 μm^3. There are significant increases in both volume and area of mPSDs 6 h after the induction of LTP ($P<0.001$). (C) Distribution of volume of Msps in control and potentiated tissue. The volumes of Msps, computed from 3D reconstructions, are grouped in steps of 0.1 μm^3. Six hours after the induction of LTP there was a large and significant increase in volume and area of mushroom ($P<0.001$). (D) Distribution of volume of perforated and segmented PSDs in control and potentiated tissue. The volumes of perforated and segmented PSDs were calculated from 3D reconstructions of Msps and are grouped in steps of 0.01 μm^3. There is a significant shift to the right in the distribution of potentiated group 6 h after induction, relative to the unstimulated controls ($P<0.001$). (E) Distribution of volume of all spines in control and potentiated tissue, grouped in steps of 0.1 μm^3. LTP is accompanied by a large and significant increase in volume and area of spines ($P<0.001$). (F) Distribution of volume of all PSDs in control and potentiated tissue, grouped in steps of 0.1 μm^3. There is a significant increase in volume and area of PSDs 6 h after the induction of LTP.

the pre-synaptic contact zone becomes more convex. At the same time, Msps expand, with a larger and more concave PSD and a correspondingly more convex pre-synaptic density (Fig. 8(3)). These processes may be

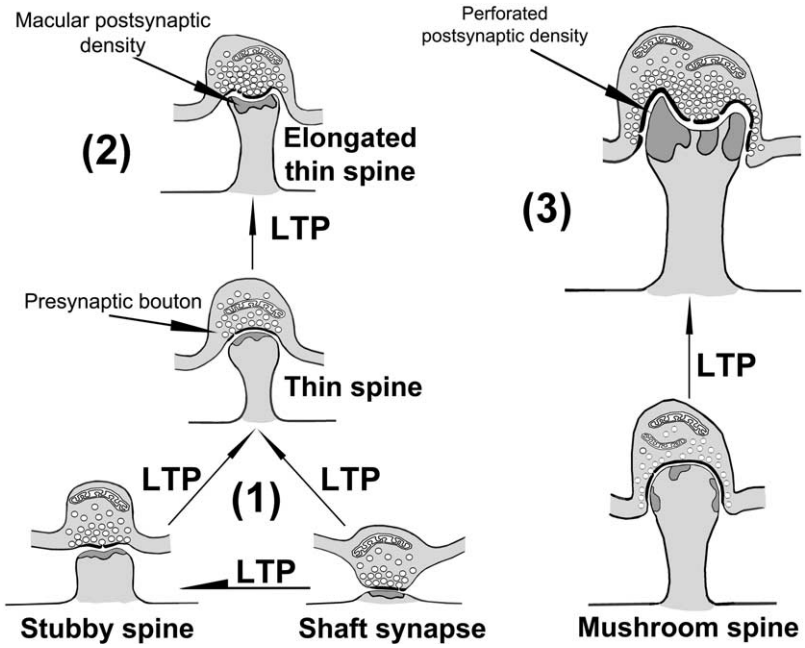

Fig. 8. Schematic interpretation of the changes in synapse and spine structure 6 h after the induction of LTP in the DG *in vivo*. Synaptic vesicles and mitochondria are shown in the pre-synaptic bouton; the PSD is dark grey at the head of the spines. Stubby spines and shaft synapses are transformed into Tsps (1), whilst existing Tsps grow larger and acquire concave heads (2). As a consequence, Tsps grow more numerous, whilst stubby spines and shaft synapses decline in number. Msp heads also become more concave (3), with no change in density but there is an increase in the PSD volume.

reversible in the absence of stimulation or in physiological conditions such as hibernation (Popov and Bocharova, 1992; Popov et al., 1992, 2003). The idea of a possible transition of shaft to stubby synapses, and stubby to thin synapses, is consistent with earlier *in vitro* and *in vivo* studies in area CA1 (Fiala et al., 1998; Kirov and Harris, 1999; Harris et al., 2003). Our findings would suggest that in the DG of the intact animal 6 h post-induction, there is remodelling of pre-existing synapses rather than splitting of dendritic spines and formation of new synapses. We did not observe an increase in the proportion of perforated/segmented synapses as reported for DG by Geinisman et al. (1992) or in the work of Muller et al. (2000). However, it is possible that the discrepancy may be explained by the different post-induction intervals at which the various studies were performed. The studies by Geinisman et al. (1992) were carried out more than 24 h post-initial LTP induction. In ex vivo studies in area CA1 by Muller et al. (2000) and Toni et al. (1999, 2001) an increase in the proportion of perforated PSDs was reported at 30 min post-tetanus, but there was a return to control levels 2 h later.

The EM data presented here only partially support the many recent confocal microscope studies and high-resolution time-lapse imaging of hippocampal tissue, which have revealed the remarkable plasticity and motility of dendritic spines both during development (Dunaevsky and Mason, 2003), and after LTP (Engert and Bonhoeffer, 1999; Maletic-Savatic et al., 1999; Nikonenko et al., 2002). We have not found evidence for an increase in spine formation reported in the latter studies; our data are in broad agreement with the work of Harris and her colleagues (1999a,b; Kirov and Harris, 1999; Ostroff et al., 2002; Sorra and Harris, 1998) in area CA1, and with the confocal microscope study of Hosokawa et al. (1995), also in area CA1, in which spine size and number were examined in acute hippocampal slices before and after chemically induced LTP. The latter experiments suggested that one of the major forms of structural change involves growth of a subpopulation of small spines, consonant with our finding of an increase in the proportion of long thin spines. Our results are also consistent with the observations of Emptage et al. (2003) who failed to find new spine or filopodia formation following an imaging study of LTP at individual spines in areas CA1 and CA3 of organotypic slices.

Recent studies have provoked a major shift in our understanding of the dendritic spine, from a stable storage site of long-term memory to a dynamic structure which is capable of undergoing rapid morphological variations (Segal and Andersen, 2001). The possibility that spine motility could also contribute to the anchoring or removing of glutamate receptors at spine heads, and may control the efficacy of existing synapses has also been discussed by Segal and Andersen (2001). Whilst the precise mechanism of spine and synapse remodelling remains unclear, it seems likely that it is closely correlated with a change in synaptic strength following stimulation (Nikonenko et al., 2002). A common mechanism involving changes in intracellular Ca^{2+} concentration may control both formation/elongation and pruning/retraction of spines (Segal 2001; Goldin et al., 2001). LTP may also involve activation of

protein synthesis on polyribosomes located in dendrites (Steward and Schuman, 2001; Ostroff et al., 2002; Goldin and Segal, 2003; Bradshaw et al., 2003), and a later phase associated with an enhanced F-actin content within the dendritic spine (Fukazawa et al., 2003). The role of actin appears to be to maintain stability of synaptic structure (Halpain et al., 1998), a stability which is disrupted by the intense glutamate receptor activity following induction of LTP. It is also possible that the remodelling of spines reflects a redistribution of synapses, since a single bouton may innervate more than one spine (Toni et al., 1999; Geinisman et al., 2001). An increase in the proportion of longer thin spines would increase the surface area available for such contacts whilst leaving the overall number of synapses of the MML unchanged. In addition longer thin spines could reach more distant axons. Such structural modifications could underlie the alterations in synaptic efficacy seen in LTP.

In summary, the quantitative 3D data presented here argue that morphological changes 6 h after the induction of LTP in the DG of the anaesthetised rat reflect synapse and dendritic spine remodelling rather than a change in the overall number of synapses.

Acknowledgments—This work was supported in part by grants BBSRC 108/S08513 and BBSRC 108/NEU15416 (to M.G.S) and The Leverhulme Trust (grant F00269G) and Russian Foundation for Basic Research (grant 48890a to V.I.P.). We thank Dr. John C. Fiala (Boston University, Boston, MA, USA) for consultations on use of the IGL Trace programme, and for helpful comments on the manuscript

REFERENCES

Abraham WC, Logan B, Greenwood JM, Dragunow M (2002) Induction and experience dependent consolidation of stable long-term potentiation lasting months in the hippocampus. J Neurosci 22:9626–9634.

Bliss TVP, Collingridge GL (1993) A synaptic model of memory: long-term potentiation in the hippocampus. Nature 361:31–39.

Bliss TVP, Lømo T (1973) Long-lasting potentiation of synaptic transmission in the dentate area of the anaesthetized rabbit following stimulation of the perforant path. J Physiol (Lond) 232:331–356.

Bradshaw, KD, Emptage, NJ, Bliss, TVP (2003) A role for local protein synthesis is required for hippocampal late LTP. Eur J Neurosci 11:3150–3152.

Chang FL, Greenough WT (1984) Transient and enduring morphological correlates of synaptic activity and efficacy change in the rat hippocampal slice. Brain Res 309:35–46.

Coggeshall RE, Lekan HA (1996) Methods for determining numbers of cells and synapses: a case for more uniform standards of review. J Comp Neurol 364:6–15.

Desmond N, Levy WB (1983) Synaptic correlates of associative potentiation/depression: an ultrastructural study in the hippocampus. Brain Res 265:21–30.

Desmond N, Levy WB (1986a) Changes in the numerical density of synaptic contacts with long-term potentiation in the hippocampal dentate gyrus. J Comp Neurol 253:466–475.

Desmond N, Levy WB (1986b) Changes in the postsynaptic density with long-term potentiation in the dentate gyrus. J Comp Neurol 253:476–482.

Desmond N, Levy WB (1988) Synaptic interface surface area increases with long-term potentiation in the hippocampal dentate gyrus. Brain Res 453:308–314.

Desmond N, Levy WB (1990) Morphological correlates of long-term potentiation imply the modification of existing synapses, not synaptogenesis, in the hippocampal dentate gyrus. Synapse 5:139–143.

Dhanrajan TM, Lynch MA, Kelly A, Popov VI, Rusakov DA, Stewart MG (2003) Expression of long term potentiation in aged rats involves perforated synapses but dendritic spine branching results from high frequency stimulation alone. Hippocampus 14:255–264.

Dunaevsky A, Mason CA (2003) Spine motility: a means towards an end? Trends Neurosci 26:155–160.

Emptage NJ, Reid CA, Fine A, Bliss TVP (2003) Optical quantal analysis reveals a presynaptic component of LTP at hippocampal Schaffer-associational synapses. Neuron 38:797–804.

Engert F, Bonhoeffer T (1999) Dendritic spine changes associated with hippocampal long-term synaptic plasticity. Nature 399:66–70.

Fiala JC, Harris KM (2001a) Extending unbiased stereology of brain ultrastructure to three-dimensional volumes. J Am Med Inform Assoc 8:1–16.

Fiala JC, Harris KM (2001b) Cylindrical diameters method for calibrating section thickness in serial electron microscopy. J Microsc 202:468–472.

Fiala JC, Feinberg M, Popov V, Harris KM (1998) Synaptogenesis via dendritic filopodia in developing hippocampal area CA1. J Neurosci 18:8900–8911.

Frey U, Krug M, Reymann KG, Matthies H (1988) Anisomycin, an inhibitor of protein synthesis, blocks late phases of LTP phenomena in the hippocampal CA1 region in vitro. Brain Res 452:57–65.

Frey U, Morris RGM (1997) Synaptic tagging and long-term potentiation. Nature 385:533–536.

Fukazawa Y, Saitoh Y, Ozawa F, Ohta Y, Mizuno K, Inokuchi K (2003) Hippocampal LTP is accompanied by enhanced F-actin content within the dendritic spine that is essential for late LTP maintenance in vivo. Neuron 38:447–460.

Geinisman Y, DeToledo-Morrell L, Morrell F, Persina IS, Rossi M (1992) Structural synaptic plasticity associated with the induction of long-term potentiation is preserved in the dentate gyrus of aged rats. Hippocampus 2:445–456.

Geinisman Y, DeToledo-Morrell L, Morrell F (1991) Induction of long-term potentiation is associated with an increase in the number of axospinous synapses with segmented postsynaptic densities. Brain Res 566:77–88.

Geinisman Y, DeToledo-Morrell L, Morrell F (1994) Comparison of structural synaptic modifications induced by long-term potentiation in the hippocampal dentate gyrus of young and aged rats. Ann NY Acad Sci 747:452–466.

Geinisman Y, Berry RW, Disterhoft JF, Power JM, Van der Zee EA (2001) Associative learning elicits the formation of multiple-synapse boutons. J Neurosci 21:5568–5573.

Goldin M, Segal M, Avignone E (2001) Functional plasticity triggers formation and pruning of dendritic spines in cultured hippocampal networks. J Neurosci 21:186–193.

Goldin M, Segal M (2003) Protein kinase C and ERK involvement in dendritic spine plasticity in cultured rodent hippocampal neurons. Eur J Neurosci 17:2529–2539.

Halpain S, Hipolito A, Saffer L (1998) Regulation of F-actin stability in dendritic spines by glutamate receptors and calcineurin. J Neurosci 18:9835–9844.

Harris KM (1994) Serial electron microscopy as an alternative or complement to confocal microscopy for the study of synapses and dendritic spines in the central nervous system. In: Three-dimensional confocal microscopy; volume investigation of biological specimens (Stevens JK, Mills LR, Trogadis JE, eds), pp 421–445. New York: Academic Press.

Harris KM (1999a) Calcium from internal stores modifies dendritic spine shape. Proc Natl Acad Sci USA 96:12213–12215.

Harris KM (1999b) Structure, development, and plasticity of dendritic spines. Curr Opin Neurobiol 9:343–348.

Harris KM, Fiala JC, Ostroff L (2003) Structural changes at dendritic spine synapses during long-term potentiation. Philos Trans R Soc Lond B Biol Sci 358:745–748.

Hosokawa T, Rusakov DA, Bliss TV, Fine A (1995) Repeated confocal imaging of individual dendritic spines in the living hippocampal slice: evidence for changes in length and orientation associated with chemically induced LTP. J Neurosci 15:5560–5573.

Kirov SA, Harris KM (1999) Dendrites are more spiny on mature hippocampal neurons when synapses are inactivated. Nat Neurosci 2:878–883.

Korkotian E, Segal M (2001) Regulation of dendritic spine motility in cultured hippocampal neurons. J Neurosci 21:6115–6124.

Malenka RC, Nicoll RA (1999) Long-term potentiation: a decade of progress? Science 285:1870–1874.

Maletic-Savatic M, Malinow R, Svoboda K (1999) Rapid dendritic morphogenesis in CA1 hippocampal dendrites induced by synaptic activity. Science 283:1923–1927.

Marrone DF, Petit TL (2002) The role of synaptic morphology in neural plasticity: structural interactions underlying synaptic power. Brain Res Rev 38:291–308.

Mezey S, Doyère V, Souza I, Harrison E, Cambon C, Kendal CE, Davies HA, Laroche S, Stewart MG (2004) Long-term synaptic morphometry changes after induction of LTP and LTD in the dentate gyrus of awake rats are not simply mirror phenomena. Eur J Neurosci 19:2310–2318.

Moser MB, Trommald M, Egeland T, Andersen P (1997) Spatial training in a complex environment and isolation alter the spine distribution differently in rat CA1 pyramidal cells. J Comp Neurol 380:373–381.

Muller D, Toni N, Buchs P-A (2000) Spine changes associated with long-term potentiation. Hippocampus 10:596–604.

Nikonenko I, Jourdain P, Alberi S, Toni N, Muller D (2002) Activity-induced changes of spine morphology. Hippocampus 12:585–591.

Ostroff LE, Fiala JC, Allwardt B, Harris KM (2002) Polyribosomes redistribute from dendritic shafts into spines with enlarged synapses during LTP in developing rat hippocampal slices. Neuron 35:535–545.

Pakkenberg B, Gundersen HJ (1997) Neocortical neuron number in humans: effect of sex and age. J Comp Neurol 384:312–320.

Peters A, Kaiserman-Abramof IR (1970) The small pyramidal neuron of the rat cerebral cortex: the perikaryon, dendrites, and spines. J Anat 127:321–356.

Petukhov VV, Popov VI (1986) Quantitative analysis of ultrastructural changes in synapses of the rat hippocampal field CA3 in vitro in different functional states. Neuroscience 18:823–835.

Popov VI, Bocharova LS (1992) Hibernation-induced structural changes in synaptic contacts between mossy fibres and hippocampal pyramidal neurons. Neuroscience 48:53–62.

Popov VI, Bocharova LS, Bragin AG (1992) Repeated changes of dendritic morphology in the hippocampus of ground squirrels in the course of hibernation. Neuroscience 48:45–51.

Popov VI, Medvedev NI, Rogachevskii VV, Ignat'ev DA, Stewart MG, Fesenko EE (2003) Three-dimensional organization of synapses and astroglia in the hippocampus of rats and ground squirrels: new structural and functional paradigms of the synapse function. Biofizika 48:289–308.

Rusakov DA, Richter-Levin G, Stewart MG, Bliss T (1997) Reduction in spine density associated with long-term potentiation in the dentate gyrus suggests a spine fusion-and-branching model of potentiation. Hippocampus 7:489–500.

Segal M (2001) Rapid plasticity of dendritic spine: hints to possible functions? Prog Neurobiol 63:61–70.

Segal M, Andersen P (2001) Dendritic spines shaped by synaptic activity. Curr Opin Neurobiol 10:582–586.

Sorra KE, Harris KM (1998) Stability in synapse number and size at 2 h after long-term potentiation in hippocampal area CA1. J Neurosci 15:658–671.

Sorra KE, Fiala JC, Harris KM (1998) Critical assessment of the involvement of perforations, spinules, and spine branching in hippocampal synapse formation. J Comp Neurol 398:225–240.

Steward O, Schuman EM (2001) Protein synthesis at synaptic sites on dendrites. Ann Rev Neurosci 24:299–325.

Stewart MG, Harrison E, Rusakov DA, Richter-Levin G, Maroun M (2000) Re-structuring of synapses 24 hours after induction of long-term potentiation in the dentate gyrus of the rat hippocampus in vivo. Neuroscience 100:221–227.

Stuart DA, Oorschot DE (1995) Embedding, sectioning, immunocytochemical and stereological methods that optimise research on the lesioned adult rat spinal cord. J Neurosci Methods 61:5–14.

Swanson LW (1998) Brain maps: structure of the rat brain. Amsterdam: Elsevier.

Toni N, Buchs P-A, Nikonenko I, Bron CR, Muller D (1999) LTP promotes formation of multiple spine synapses between a single axon terminal and a dendrite. Nature 402:421–425.

Toni N, Buchs P-A, Nikonenko I, Povilaitite P, Parisi L, Muller D (2001) Remodelling of synaptic membranes after induction of long-term potentiation J Neurosci 15:6245–6251.

Weeks AC, Ivanco TL, Leboutillier JC, Racine RJ, Petit TL (1999) Sequential changes in the synaptic structural profile following long-term potentiation in the rat dentate gyrus: I. The intermediate maintenance phase. Synapse 31:97–107.

Weeks A, Ivanco T, LeBoutillier J, Racine R, Petit T (2000) Sequential changes in the synaptic structural profile following long-term potentiation in the rat dentate gyrus. II. Induction/early maintenance phase. Synapse 36:286–296.

Weeks A, Ivanco T, LeBoutillier J, Racine R, Petit T (2001) Sequential changes in the synaptic structural profile following long-term potentiation in the rat dentate gyrus. III. Long-term maintenance phase. Synapse 40:74–84.

Weeks AC, Ivanco TL, Leboutillier JC, Marrone DF, Racine RJ, Petit TL (2003) Unique changes in synaptic morphology following tetanization under pharmacological blockade. Synapse 47:77–86.

Yuste R, Bonhoeffer T (2001) Morphological changes in dendritic spines associated with long-term synaptic plasticity. Annu Rev Neurosci 24:1071–1089.

Zakharenko SS, Zablow L, Siegelbaum SA (2001) Visualization of changes in presynaptic function during long-term synaptic plasticity. Nat Neurosci 4:711–717.

(Accepted 16 June 2004)
(Available online 20 August 2004)